A density functional for sparse matter

2009 J. Phys.: Condens. Matter 21 084203

(http://iopscience.iop.org/0953-8984/21/8/084203)

J. Phys.: Condens. Matter **21** (2009) 084203 (15pp) doi:10.1088/0953-8984/21/8/084203

A density functional for sparse matter

D C Langreth[1], B I Lundqvist[2,3], S D Chakarova-Käck[2], V R Cooper[1], M Dion[1], P Hyldgaard[4], A Kelkkanen[3], J Kleis[2,3], Lingzhu Kong[1], Shen Li[1], P G Moses[3], E Murray[1], A Puzder[1], H Rydberg[2], E Schröder[2] and T Thonhauser[1]

[1] Center for Materials Theory, Department of Physics and Astronomy, Rutgers University, Piscataway, NJ 08854-8019, USA
[2] Department of Applied Physics, Chalmers University of Technology, SE-41296 Göteborg, Sweden
[3] Center for Atomic-scale Materials Design, Department of Physics, Technical University of Denmark, DK-2800 Kongens Lyngby, Denmark
[4] Department of Microtechnology and Nanoscience, Chalmers University of Technology, SE-41296 Göteborg, Sweden

Received 30 July 2008, in final form 28 September 2008
Published 30 January 2009
Online at stacks.iop.org/JPhysCM/21/084203

Abstract
Sparse matter is abundant and has both strong local bonds and weak nonbonding forces, in particular nonlocal van der Waals (vdW) forces between atoms separated by empty space. It encompasses a broad spectrum of systems, like soft matter, adsorption systems and biostructures. Density-functional theory (DFT), long since proven successful for dense matter, seems now to have come to a point, where useful extensions to sparse matter are available. In particular, a functional form, vdW-DF (Dion *et al* 2004 *Phys. Rev. Lett.* **92** 246401; Thonhauser *et al* 2007 *Phys. Rev.* B **76** 125112), has been proposed for the nonlocal correlations between electrons and applied to various relevant molecules and materials, including to those layered systems like graphite, boron nitride and molybdenum sulfide, to dimers of benzene, polycyclic aromatic hydrocarbons (PAHs), doped benzene, cytosine and DNA base pairs, to nonbonding forces in molecules, to adsorbed molecules, like benzene, naphthalene, phenol and adenine on graphite, alumina and metals, to polymer and carbon nanotube (CNT) crystals, and hydrogen storage in graphite and metal–organic frameworks (MOFs), and to the structure of DNA and of DNA with intercalators. Comparison with results from wavefunction calculations for the smaller systems and with experimental data for the extended ones show the vdW-DF path to be promising. This could have great ramifications.

(Some figures in this article are in colour only in the electronic version)

1. Introduction

By sparse matter we mean systems with important regions having very low electron density. It is exemplified by soft matter (figure 1), biological matter, nanostructures, corrosion and catalyst layers. Both strong local bonds and weak nonbonding forces are important. In particular, the nonlocal correlations behind the van der Waals (vdW) forces between atoms separated by empty space is a ubiquitous and often important phenomenon. Examples of such matter are found in vdW molecules, soft matter, molecule adsorption systems and biostructures.

For dense matter, density-functional theory (DFT) has well proven its usefulness to account for structure, cohesion and other static properties. Today the standard DFT approach involves the general-gradient approximation (GGA), particularly successful for describing valence bonds. To extend DFT's usefulness to the large classes of matter with *both* high-density chunks and low-density regions, a general density functional that includes vdW interactions is very desirable.

Soft matter is abundant in nature. It encompasses solids, like graphite, molecular crystals, and polymers, liquids and macromolecular systems, interacting systems, like in adsorption, water overlayers and hydrogen storage, biostructures, like DNA, protein structure and protein folding, and numerous other sparse systems surrounding us in our daily lives, like bread, butter, cheese, grease, tissues, tape, paint, dust, rust, cloth, plastics, snowflakes, ski wax, leaves and

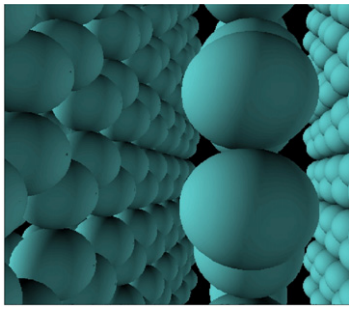

Figure 1. Sparse matter: model of graphite [1].

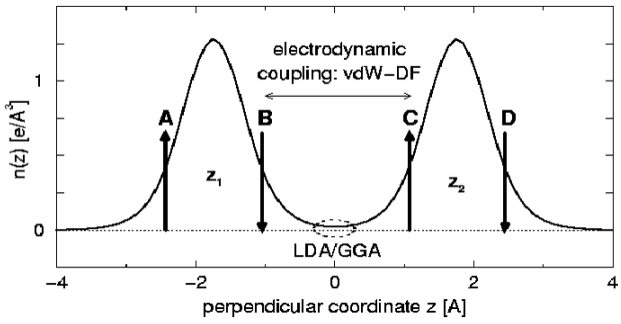

Figure 2. Schematic account of vdW forces in sparse, layered matter (two graphene sheets at equilibrium separation) [2]. Towards a background of laterally averaged electron density, the vertical arrows mark typical locations of charge fluctuations, the horizontal arrow the region of correlation between them and the dotted ellipse the very different region of relevance for GGA (and LDA).

flowers. With perspectives of condensed-matter theorists and surface and materials theoreticians, after crucial development and the work of many [1], we have proposed such a functional (vdW-DF) [2, 3].

In this paper the background and basis for vdW-DF are briefly reviewed, as are the growing number of applications of it. The outcome of these applications is assessed, and the anticipations for the future are expressed.

2. van der Waals forces

van der Waals (vdW) interactions, also known as London dispersion interactions, constitute a quantum-mechanical phenomenon with charge fluctuations in one part of an atomic system that are electrodynamically correlated with charge fluctuations in another. The system experiences this as an attractive vdW force (figure 2). The vdW force at one point thus depends on charge events at another region and is a truly nonlocal correlation effect.

3. van der Waals interactions in DFT

The exact density functional [4, 5] contains the vdW forces [6]. Unfortunately, we do not have access to the exact DFT. Approximate versions are abundant, however. Commonly, the local-density approximation (LDA) [5, 7–11] and the general-gradient approximation (GGA) [12–18] are used. They depend on the density in local and semilocal ways, respectively, however, and give no account of the nonlocal vdW interaction (figure 2).

There are empirical and semi-empirical accounts for the vdW or London dispersion forces that rely on the asymptotical form $-1/d^4$ for insulating sheets of boron nitride (for example) and $-1/r^6$ for atoms and molecules. The correct values of these forces at important distances like vdW bond lengths are substantially different from those predicted by the asymptotic forms.

Today there are proposals for how the vdW *can* be treated in DFT, in particular at large separations [19–21]. We have proposed functionals for all separations, one for layered systems [1] and one for general geometries [2, 3]. They are both developed in the same spirit but differ in detail. The earlier functional [1] relied on lateral averaging to render the charge-density truly planar and is considered only of historical importance as it gave guidance to the construction of the general-geometry functional [2, 3], which after all can be used on layered systems as well.

In DFT, the electron density $n(r)$ is the key quantity, and the energy functional can be expressed as [5]

$$E[n] = T_s[n] + V_{ee}[n] + V_{ion}[n] + E_{xc}[n], \qquad (1)$$

where the first three terms are the functionals for the kinetic energy of noninteracting electrons, the Coulomb energy of the electrons and the interaction energy between electrons and ions, respectively. The remaining term, $E_{xc}[n]$, the exchange–correlation energy functional, contains all the interactions for which there is no exact functional.

However, there is a so-called adiabatic-connection formula that provides a formal basis for $E_{xc}[n]$, a recipe for how approximate exchange–correlation energy functionals can be generated [22, 23, 10]. The 'standard' DFT calculations today typically use the local LDA or the semilocal GGA for $E_{xc}[n]$, with quite some success for dense matter, including hard materials and covalently bound molecules.

4. Density functional in vdW-DF

The vdW-DF procedure is in short

$$E_{xc}[n] = E_x^{GGA}[n] + E_c^{new}[n], \qquad (2)$$

that is (i) to take an appropriately selected GGA exchange functional, (ii) to develop a properly constructed *nonlocal* correlation functional that includes an account of vdW forces and (iii) to perform calculations with some efficient and accurate electron-structure scheme, for instance, with plane-wave and real-space codes. The computer resources required for vdW-DF [2] are comparable to ordinary DFT (e.g. GGA). By using the functional derivative of $E_c^{new}[n]$ with respect to the density $n(r)$ as a component of the Kohn–Sham electron potential [5], the calculations are made fully self-consistent [3].

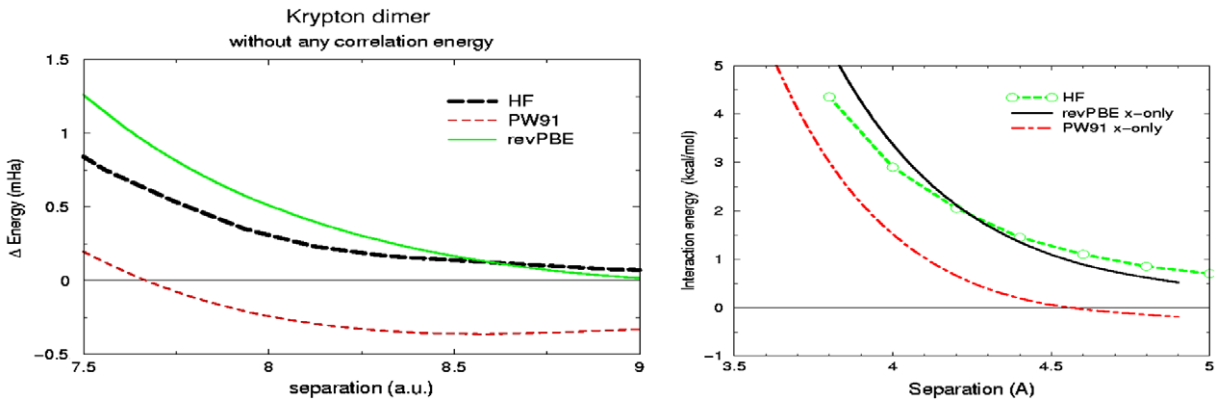

Figure 3. Variation of exchange functionals and exact Hartree–Fock (HF) with separation for the krypton (left) [26] and benzene dimers (right) [27].

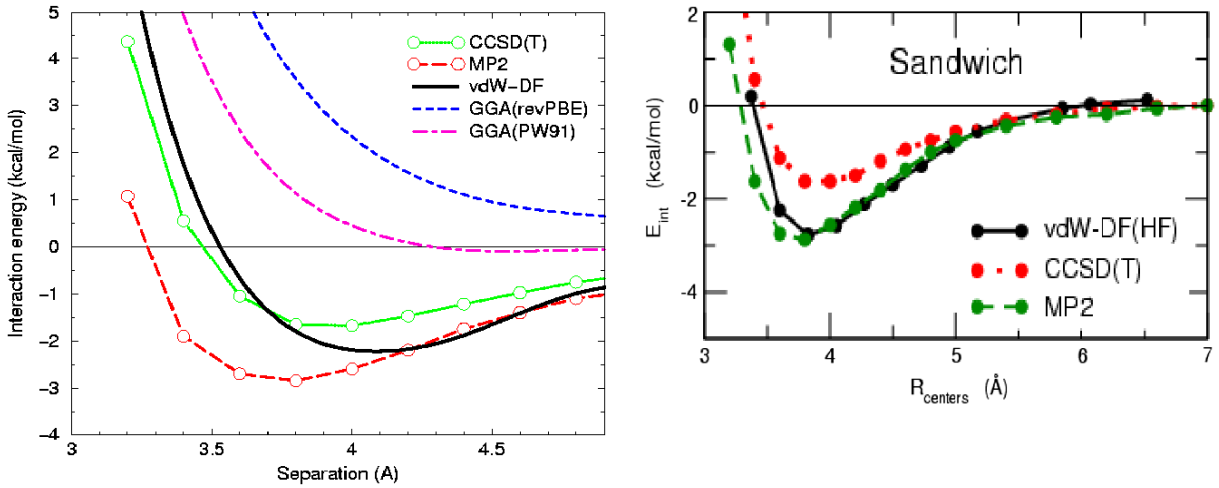

Figure 4. Binding-energy calculations for the benzene dimer in various approximations [2, 27].

4.1. Exchange

Among approximation schemes for the *exchange* energy, many standard GGA flavors give substantial 'vdW' binding from *exchange* alone [24]! Exact exchange calculations in some test cases, like those in figure 3, show this behavior to be incorrect. From such comparisons (figure 3), we find that the revPBE flavor of GGA exchange [25] has less of this problem and was closer to Hartree–Fock (figure 3). Therefore, we chose revPBE exchange. The successes of LDA and GGA stem from their accounts of exchange and correlation in high-density regions, important for the covalent bond. Less attention has been given to the low-density regions in the tails of the electron distribution. This might be a reason for the spread between different flavors of GGAs in the tails. One should note that PW91 [16] exchange is an extreme case, and the more recent PBE [18] functional gives curves closer to HF, but still with an attractive part.

The ultimate exchange functional, the exact Hartree–Fock (HF) exchange, is possible to use, in particular for small systems. It has been explored for dimers of benzene [27], where it gives improved values for the equilibrium separation values but larger values for the binding energy [27]. Similar results have recently been presented in [28]. Values of the vdW bond lengths that are a couple of per cent too large seem to be the rule in the vdW-DF results reviewed below. It is good to know the cause of this and to know a possible remedy for it that can be used, at least in principle. Still, it is important to realize that there is a cancellation of errors between exchange and correlation in DFT, and that it is normally important to have a match between the exchange and correlation functionals used. This means that comparison of the exchange functional with HF is not necessarily the most effective test.

For the benzene dimer (figure 4), an HF calculation is a realistic option, as one can test the use of HF exchange instead of revPBE exchange in a vdW-DF calculation. For the sandwich configuration, the resulting potential-energy curve (PEC) is similar, but the bond length is much better, the sandwich structure is a saddle point in the energy landscape and the binding is stronger, even stronger than the 'best' wavefunction-method result (CCSD(T)) [27].

Needless to say, these short-range interactions should be worried about, including the urgent problem of improving the exchange functional, but this would involve testing on a great number of non-vdW systems. As this paper illustrates, the large number of interesting vdW systems around us has

made us give priority to *applications* of the proposed vdW-DF, knowing well the limitations in the revPBE [25] account of the exact exchange. Results similar to those for the benzene dimer apply for other test systems. The revPBE exchange is chosen because it best eliminates the spurious bonding from exchange alone, but the fact that it is not perfect is reflected in the slightly longer bonds obtained with it. Nevertheless it has proved a good match for the vdW-DF correlation functional in giving better equilibrium energies than when HF exchange is used. The search for an improved exchange functional has high priority.

4.2. Correlation

The correlation energy is split into shorter-and longer-ranged parts:

$$E_c[n] = E_c^o[n] + E_c^{nl}[n]. \tag{3}$$

The short-ranged term, $E_c^o[n]$, is evaluated in LDA, which implicitly uses the exact dielectric function. The longer-ranged part, E_c^{nl}, depends nonlocally on the density and contains the principal vdW terms. It is also much smaller in magnitude and in positional sensitivity, so it can be evaluated with a lower accuracy. In particular, in the vdW-DF it is evaluated with a simple model dielectric function.

As a matter of fact, in the vdW-DF [2], the key ingredients of this long-range (nonlocal) part of the correlation functional are (i) the adiabatic-connection formula [22, 23, 10] as the starting point, (ii) an approximate coupling-constant integration, (iii) which as in the planar case [1] is exact for the asymptotic long-range vdW term, (iv) the use of an approximate dielectric function ε in a single-pole form, (v) which is fully nonlocal and satisfies known limits, sum rules and invariances, (vi) whose pole position is scaled to give the exact electron-gas ground-state energy locally, including the appropriate gradient correction (the pole strength is determined by a sum rule) and (vii) the lack of empirical or fitted parameters.

The coupling-constant (λ) integration in the nonlocal correlation term $E_c^{nl}[n]$ in equation (3) is performed by making the simplest of approximations:

$$(\varepsilon - 1)_\lambda = \left[\frac{(\varepsilon - 1)}{\lambda}\right]_{\lambda=1} \lambda \tag{4}$$

as this can be shown to give the longest-range van der Waals terms exactly, if long-range 'spectator' interactions are also left out of the dielectric function (as they implicitly are in our simple model) [2]. A thorough discussion of this issue has been given by Dion [29]. This secures the proper asymptotic dependence. For intermediate separations its accuracy is tested in a large number of applications and comparisons with accurate results of wavefunction methods and/or experimental results, whenever such results are available. While singular in the well-known asymptotic form at large separations, the vdW interaction given by vdW-DF at small separations gives a saturation of the interaction. This is guaranteed by the form of the kernel (figure 5).

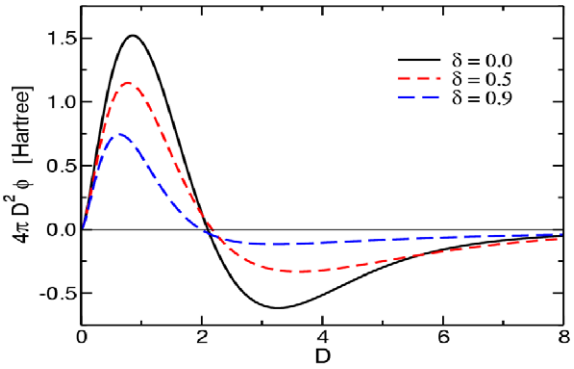

Figure 5. The kernel in equation (5) as a function of the dimensionless separation parameter D for several values of the asymmetry parameter δ, both parameters defined in the text.

The form of the general-geometry functional for $E_c^{nl}[n]$ derived in [2] is

$$E_c^{nl} = \tfrac{1}{2} \int d^3r \int d^3r'\, n(\boldsymbol{r}) \Phi(\boldsymbol{r}, \boldsymbol{r}') n(\boldsymbol{r}') \tag{5}$$

where $\Phi(\boldsymbol{r}, \boldsymbol{r}') = \Phi(q(\boldsymbol{r}), q(\boldsymbol{r}'))$. The interaction kernel depends on the density and its gradient, $q(\boldsymbol{r}) = q(n(\boldsymbol{r}), \nabla n(\boldsymbol{r}))$, and can be given a scalable form via

$$D = \frac{q + q'}{2} |\boldsymbol{r} - \boldsymbol{r}'|, \qquad \delta = \frac{1}{2} \frac{q - q'}{q + q'},$$
$$q = q(\boldsymbol{r}), \qquad q' = q(\boldsymbol{r}').$$

The kernel Φ (figure 5) is attractive at large and intermediate effective distances D. At very large D values, it takes its proper asymptotic form, and it has an oscillation at short distances D. Its repulsive part is such that the area under the solid black curve vanishes, which is the key to seamlessness and the lack of double counting [2, 26]. Double counting is avoided, as the short-range part is treated in LDA (no nonlocal component), while the long-range part has no local component, by construction, as made evident by the vanishing of the integral mentioned above.

In the self-consistent version of vdW-DF [3], there are oscillatory nonlocalities also in the exchange–correlation potential in the Kohn–Sham equations [5]:

$$V_c^{nl}(\boldsymbol{r}) = \delta E_c^{nl}[n]/\delta n(\boldsymbol{r}). \tag{6}$$

Obviously, the self-consistent version [3] is the more complete and proper one. However, the extensive computations that it calls for do not always have to be performed. Comparison of results of the self-consistent vdW-DF scheme [3] with those of the 'older' post-GGA perturbation of vdW-DF [2] typically show negligible differences. This is illustrated by the vdW binding energies of the displaced CO_2 dimer [3] and of H_2O on benzene [3, 30], with about the same results near equilibrium separations and only small differences at smaller separations (figure 6). However, there are situations, where the self-consistent version is needed very much, for instance, for Hellmann–Feynman forces in molecular-dynamics simulations [3] and for incipient charge transfer

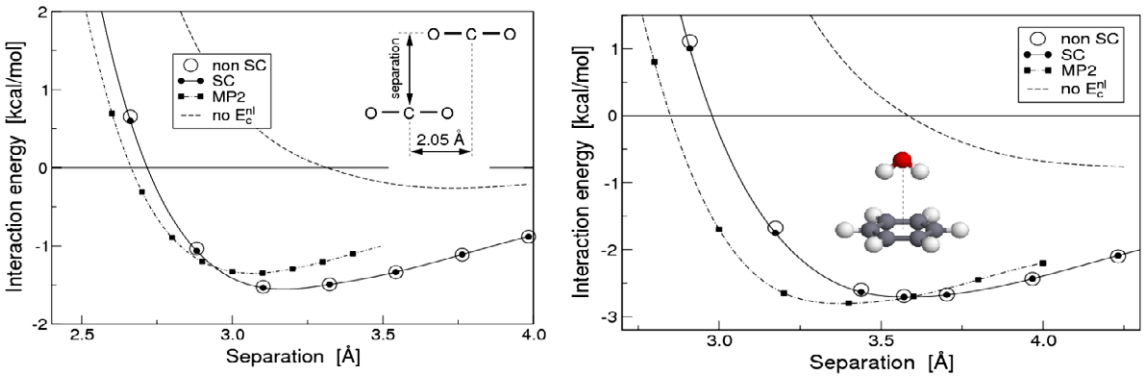

Figure 6. Self-consistent (dots) [3] and post-GGA perturbative (circles) [2] vdW-DF results for PECs of dimers of displaced parallel CO_2 molecules (left) and H_2O on top of the midpoint of a benzene molecule (right) [3]. Wavefunction-calculation (MP2) and GGA-calculation results are shown for comparison.

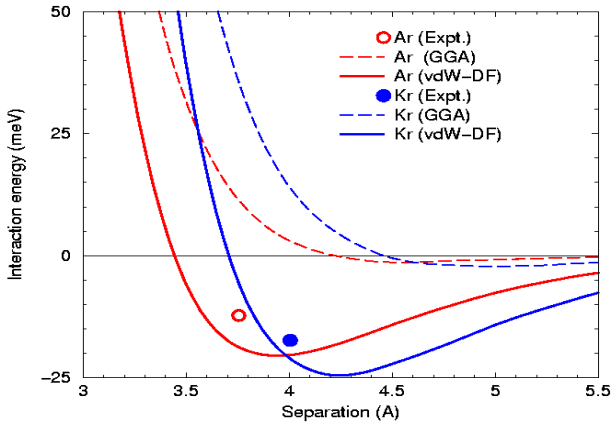

Figure 7. PECs calculated with the vdW-DF [2] (solid lines) compared with the generalized gradient approximation (GGA) (dashed lines), for the Ar (red curves starting at the left) and Kr (blue curves starting at the right) dimers. Experimental equilibrium data [40] are shown for comparison.

affected by vdW forces, as relevant for, e.g., self-assembled molecular-electronic systems.

5. Applications of vdW-DF

5.1. Atoms and molecules

The vdW-DF has been applied to dimers of atoms [2]. Results for argon and krypton dimers can be compared to experimental data (figure 7) to show the virtues and vices of the method on such localized systems. There should be better methods to obtain accurate vdW descriptions of such localized systems.

However, as vdW-DF is based on electron-gas (homogeneous and almost homogeneous) many-body results [1–3, 26], its main targets are systems with extended electron states. Among molecular systems, there are presently applications to dimers of benzene [2, 27, 31] and benzene-like molecules [32], pairs of other small molecules [3, 27, 30, 31], dimers of PAHs [41, 31], polymer interactions [43] and dimers of cytosine [3] and other DNA and RNA base-pair molecules [47]. They have typically a size that allows wavefunction calculations to be performed and thus comparisons to be made, and it is gratifying that there is a generally fair agreement between the results of the two types of methods, when comparisons are possible.

The benzene molecule has extended valence-electron states and a small energy gap. It is not jellium but closer to it than, for example, He. Further, it is generally used as a model system for vdW interaction and a prototypical system for π-electron (figure 8) interactions. The benzene dimer, this smallest aromatic system, appears in sandwich, slip parallel and T-shape configurations (figure 8), and the question, which of these configurations is stable, is still debated.

Polycyclic aromatic hydrocarbon (PAH) dimers have even more extended electron states, which make them apt for application of vdW-DF. vdW-DF calculations on PAH dimers give increased dimer binding and separation with increasing numbers of benzene rings [41, 31] (figure 9). Comparisons with equilibrium binding energy and (vertical) separation values from CCSD(T) calculations [42] are favorable, e.g. 0.247 eV/dimer and 3.5 Å for naphthalene in AB stacking, compared to 0.29 eV and 3.7 Å in the vdW-DF calculation [41, 31].

Water on aromatic molecules constitutes a small system with several types of interactions. A system with an H_2O molecule interacting with a benzene molecule involves both vdW and electrostatic forces, and could be important for understanding the hydrogen bond and adsorbed water layers. vdW-DF calculations on it [3, 30] show that the stable configuration is with the water molecule standing above or below with the H atom as shown in the right panel of figure 6. Here the water makes a hydrogen bond with the π cloud of the benzene (enhanced by London dispersion), with a vdW-DF predicted strength of 2.9 kcal mol^{-1}. This is confirmed to be the minimum energy configuration by the best MP2/CCSD(T) calculations [33–35], which give a binding energy of about 3.3 kcal mol^{-1}. The authors [30] trace out the interaction energy between water and benzene in a variety of configurations. One of the sequences considered is shown in figure 10.

This type of study can be extended to the noncovalent forces in C–H/π interactions [36]. On complexes like

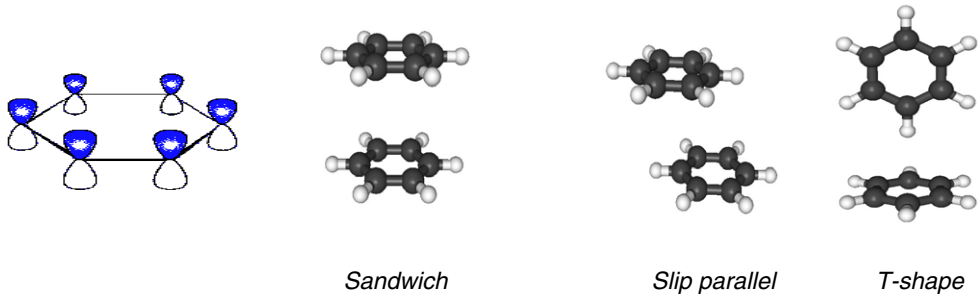

Figure 8. Schematics of the π-electron system of the benzene molecule, and some relevant structures of benzene dimers.

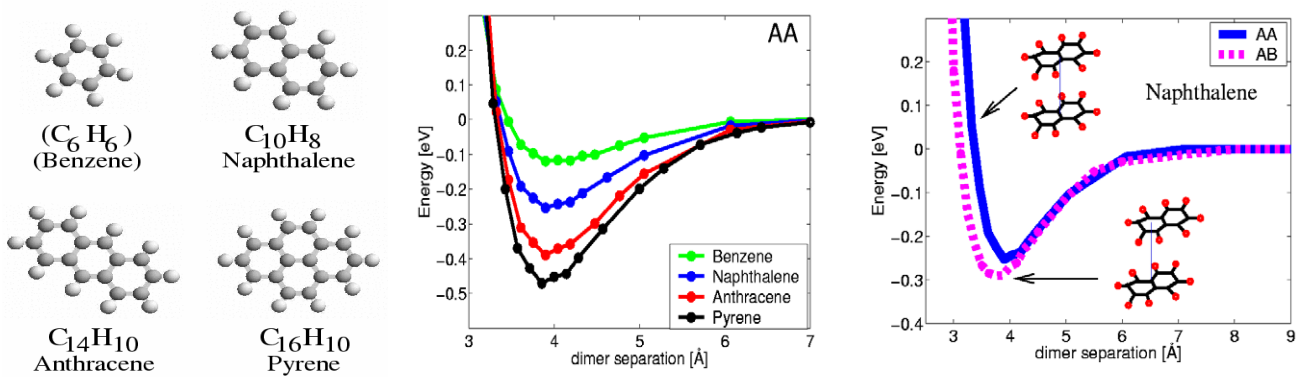

Figure 9. Polycyclic aromatic hydrocarbons (PAH) (left) and PECs of PAH dimers calculated with vdW-DF in the AA (middle) and AB (right) stackings [41, 31].

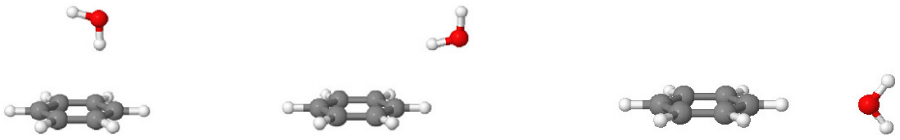

Figure 10. The optimized orientation and height of the water molecule as the horizontal coordinate of the oxygen is moved from the global minimum energy configuration (left) to a saddle point configuration (right) [30]. If instead the horizontal oxygen coordinate is moved to the left, one reaches another saddle point configuration, with the oxygen over the center of the benzene and the H atoms equidistant from the benzene plane. This latter saddle point is the lowest-energy configuration of the geometry shown in figure 6.

Table 1. Bonding results for systems with an aromatic π and an aliphatic C–H group calculated with different methods [36]. The separations R are in Å, while interaction energies E_{int} are in kcal mol^{-1}.

	C_6H_6–CH_4		C_6H_6–CHF_3		C_6H_6–$CHCl_3$		C_8H_7N–CH_4	
	R	E_{int}	R	E_{int}	R	E_{int}	R	E_{int}
vdW-DF	4.1	−1.57	3.6	−3.73	3.6	−5.11	4.0	−1.81
PBE	4.2	−0.40	3.7	−2.04	3.7	−2.07	4.2	−0.41
CCSD(T)	3.8	−1.45	3.4	−4.20	3.2	−5.60	3.8	−1.57
MP2	3.8	−1.79	3.4	−4.60	3.2	−7.20	3.7	−1.96

Figure 11. Benzene dimers with the substituents CH_3 and OH, which are electron donors. Comparison via vdW-DF with the substituents F and CN, which are electron acceptors, has allowed the effects of electronegativity to be studied [32].

methane–benzene (C_6H_6–CH_4), trifluoromethane (C_6H_6–CHF_3), trichloromethane (C_6H_6–$CHCl_3$) and methane–indole (C_6H_3N–CH_4), the vdW-DF predicts noncovalent interactions that are characterized by a weak bond between an aromatic π system and an aliphatic C–H group. The results (table 1) show significant improvement over traditional DFT and compare favorably with CCSD(T) and MP2 results [36].

With substituents like CH_3 and OH (figure 11), the variation of binding properties of benzene-like dimers with electronegativity can be studied in a systematic way [32], as OH is a strong electron donor, CH_3 an electron donor, F an electron acceptor and CN a strong electron acceptor. Doing this in sandwich (figure 12), T-shape 1 and T-shape 2 configurations gives a large database to study the effect [32, 44].

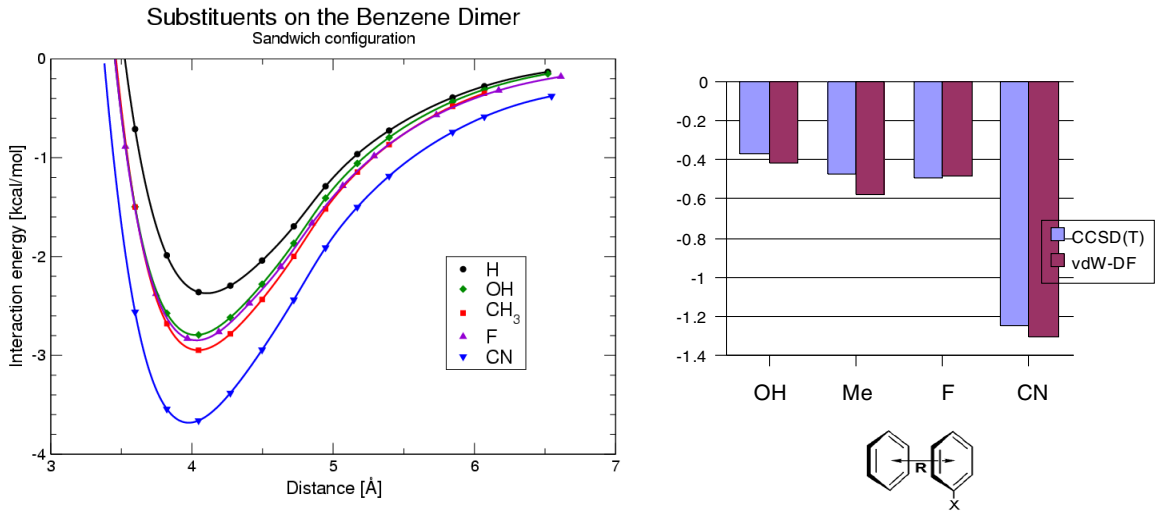

Figure 12. PECs for 'doped' benzene dimers, in sandwich configuration, calculated with vdW-DF [32] (left) and binding energy shifts from calculations in vdW-DF [32] and CCSD(T) [44] (right).

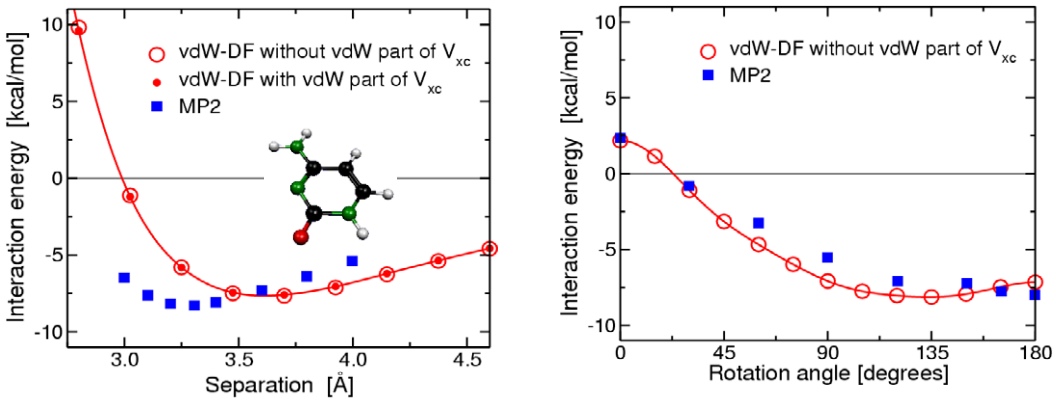

Figure 13. The PEC for the cytosine dimer composed of two parallel cytosine molecules ($C_4H_5N_3O$, shown as an inset in the left panel). The left panel gives the PEC as a function of separation at zero rotation angle, while the right panel shows the PEC as a function of rotation angle at a fixed separation of 3.4 Å. In each case the vdW-DF results [3, 47] are compared with those of wavefunction methods [46]. The left panel also shows that it is not necessary to consider the change in density that occurs when the vdW interaction is turned on, as results of self-consistent calculations (black dots [3]) and by post-GGA perturbation of vdW-DF [2] show negligible differences.

Before 2004 there was a common wisdom, based on arguments of electrostatics and exchange repulsion: 'donors increase π–π repulsion and acceptors decrease it. *Therefore acceptors increase binding energy and donors decrease it.*' However, in 2004 a wavefunction calculation [44] disproved this claim. Interaction-energy differences for the sandwich structure, i.e. doped benzene value minus benzene value (kcal/mol) are all negative! For the T-shape 1 and T-shape 2 configurations, there are also strong deviations from the old rules. Calculations with the vdW-DF give interaction-energy difference values for the twelve systems, obtained with four substitutions and three structures, the same sign and size as the CCSD(T) wavefunction calculation (figure 13 shows results in the sandwich structure; similar results are for other structures, with only F substitution in T-shape 2 differing in size) [32].

Multiple substituents in benzene in cytosine (figure 13) do not only provide a careful step further on the substitution road but point at subsequent applications on DNA and RNA. Although a many-atom system, for the cytosine dimer there are also valuable wavefunction calculations to compare with (figure 13) [3].

An attempt for a more general assessment of the accuracy of the vdW-DF versus wavefunction methods is made in table 2 [47], where binding-energy results from recent quantum-chemical (QC) calculations for the Hobza group's set S22 [35] and from the semi-empirical DFT-D method [48, 49] are given for comparison.

The comparisons in table 2 and the other favorable comparisons with wavefunction calculations for molecular systems show promise and make us believe that the vdW-DF method can be fruitfully applied to more extended systems, where wavefunction calculations are lacking.

5.2. *Crystalline solids*

Graphite is the textbook example of a vdW-bonded solid. Within the layers, sp^2-hybridized covalent bonds give a strength missing its parallel. This strength together with

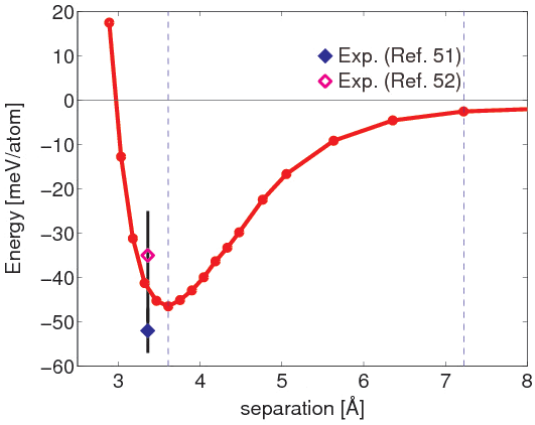

Figure 14. The PEC of a graphene dimer according to vdW-DF [45]. The interlayer binding of graphite is given by the sum of the PEC values at the two vertical dashed lines (first and second layer positions). The experimental points are derived from extrapolation of carbon nanotube (CNT) unfolding [51] and of desorption data [52].

the vdW bonds between the layers make graphite the stable carbon solid, leaving diamond as a metastable structure. The vdW-DF calculations are typically performed for two parallel graphene sheets. Thanks to the rapid decay of vdW forces with separation the binding energy between these sheets are almost equal to the interlayer binding energy. Figure 14 gives the PEC from a vdW-DF calculation [45]. While it is known that the semi-metallic nature of graphite leads to a small weakening of that asymptotic vdW interaction for these systems [50], the extent to which this may influence the interaction near the equilibrium position is unknown, and no attempt to include it was made in the calculations shown below.

For comparison with experimental results, x-ray data have long been available for the interlayer separation, which is a few per cent shorter than the calculated value. For the binding energy, actually that between two graphene sheets, the two experimental numbers that we have found are both indirect, one from extrapolation of carbon nanotube (CNT) unfolding [51] and one from extrapolation of desorption data [52].

To answer questions about the effects on hard materials, vdW-DF calculations have been performed on an Si crystal in the diamond structure, showing that the good agreement between GGA results and experiment is not hurt [3].

Table 2. Binding-energy results (kcal mol^{-1}) for characteristic noncovalently bound molecules (the Hobza group's set S22 [35]) calculated with the vdW-DF method (compiled In [47]), with quantum-chemical methods (QC) [35], and from the semi-empirical DFT-D method with BLYP-D (04) [48] and BLYP-D (07) [49].

	vdW-DF	QC	BLYP-D (04)	BLYP-D (07)
AT (WC)	−15.20	−16.37	−15.01	−17.19
Benzene-CH_4 (C_3)	−1.57	−1.50	−0.90	−1.37
Benzene-H_2O (C_s)	−2.86	−3.28		−4.16
Benzene dimer (C_{2v})	−2.28	−2.74	−2.03	−2.76
Benzene dimer (C_{2h})	−2.80	−2.73	−2.00	−2.35
AT (stack)	−9.55 [a]	−12.23	−10.47	−12.85

[a] Not geometrically optimized.

Potassium intercalation in graphite has been studied by vdW-DF [55], as an account of the intercalation formation energy from pure K atoms and graphite requires a description of the graphite interlayer binding energy and thus of the vdW forces. The vdW-DF calculation indicates that the vdW interaction supplements the ionic bond in the final intercalation compound C_8K, with key contributions to the binding separation, layer binding energy, formation energy and bulk modulus (vdW forces strengthen the interlayer binding energy of the C_8K by more than 50%, from 511 meV in GGA to 793 meV per formula unit) [55]. The vdW-DF results for structure and elastic response are in fair agreement with experiment. However, the intercalation process is predicted to leave the bulk modulus unchanged, while experiments indicate a moderate hardening [55].

The vdW-DF is of particular interest for molecular crystals. Applications have been made to crystalline polyethylene (figure 15) [53], with results close to experiment, about as close as with an empirical force-field method, and to a semiconducting CNT crystal (figure 16) [43], where vdW-DF predicts (i) an intertube bonding with a strength consistent with recent observations for the interlayer binding in graphitics (30 versus 50 meV/atom) and (ii) a CNT wall-to-wall separation (D approx. 3.45 Å) in very good agreement with experiment ($D = 3.4$ Å) [43].

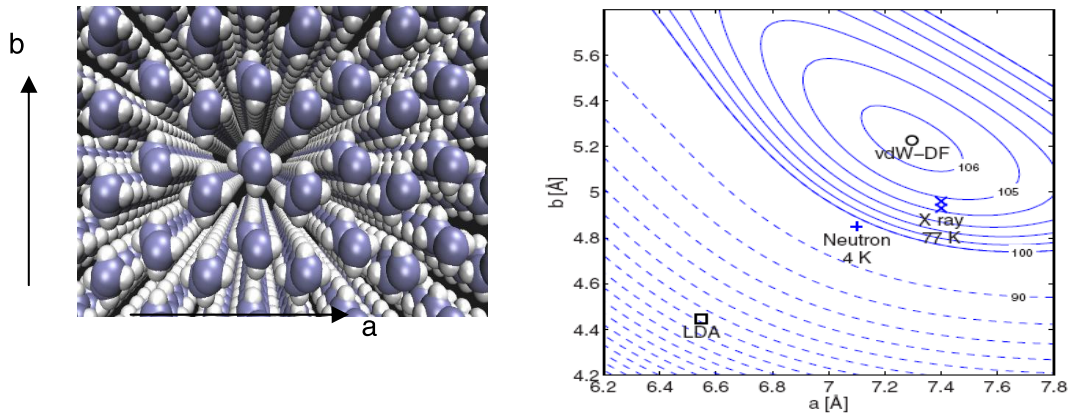

Figure 15. The polyethylene crystal and its energy landscape according to vdW-DF [53].

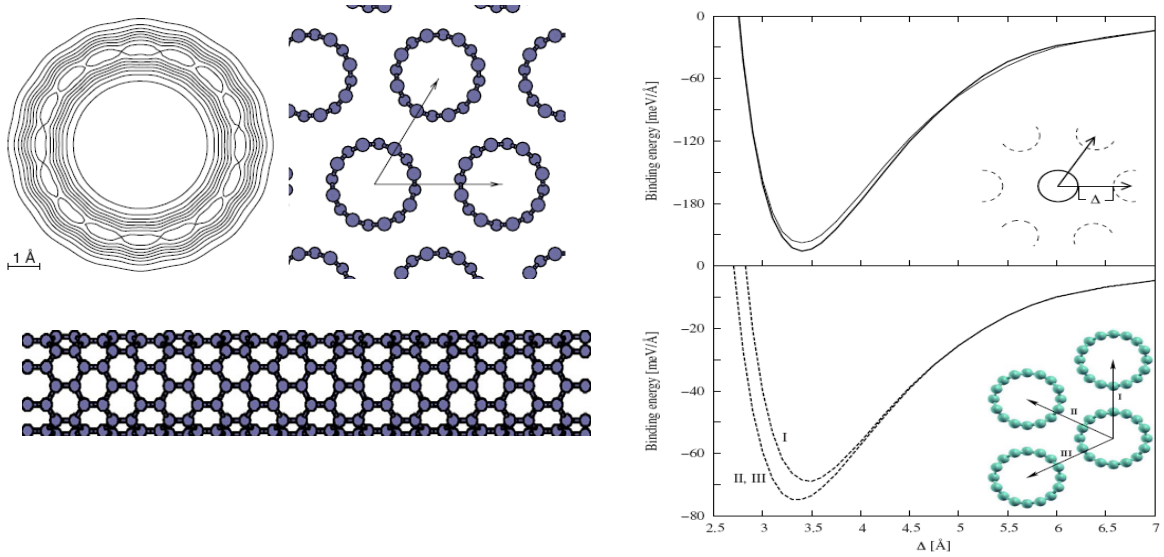

Figure 16. The semiconducting CNT crystal and its energy landscape according to vdW-DF [43].

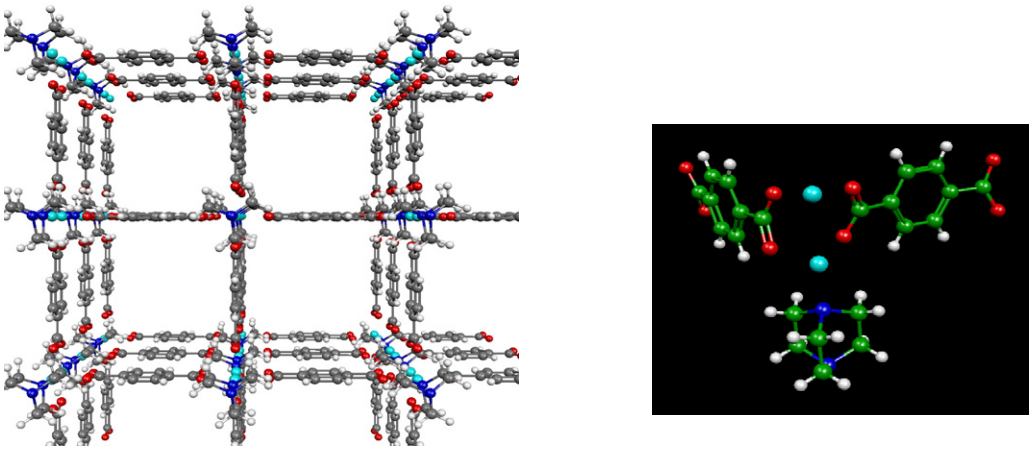

Figure 17. Example of a simple MOF structure (left) and its components, two linkers and a pillar, joined by two metal atoms (in this case Zn) (right) [56]. The H_2 is bound in several channels which are difficult to guess, but which have been calculated using vdW-DF [56].

Recent developments with the vdW-DF on molecular crystals can be exemplified by complications in connection with H_2 monolayer calculations in the mentioned problem of hydrogen storage in graphite [37, 38]. Calculational methods have to be improved to account for the many orientations of the H_2 molecule [54].

Application [56] to hydrogen storage in metal–organic frameworks (MOFs) [57, 58] clearly demonstrates the advantages of using a DFT-like vdW-DF. The components of simple MOF are metal atoms connected by organic molecule pillars and linkers (figure 17). It allows the study of the binding of H_2 to an individual linker, where the vdW-DF results for the H_2–linker interaction energy [56] can be compared with quantum-chemical results [59]. It also allows a modeling of the entire MOF, which shows differences in H_2 binding energy and binding sites between the MOF and the fragment [56]. Shifts in H_2 stretching frequency have been calculated, providing a valuable possibility of validation of the modeling [56]. Ultimately the relation of binding sites to structure will be fed back to experts [57, 58] in MOF fabrication, in the hopes of creating improved hydrogen-storage materials.

5.3. Adsorption

Molecular adsorption offers interesting possibilities to test vdW-DF results against experiment. The binding energy, or rather the adsorption or desorption energy, is directly measurable in, for example, desorption experiments. The systems studied so far include adsorbates like benzene and aromatic molecules, and a number of different planar substrates.

The vdW-DF calculation of the desorption energy for benzene from graphite [45] has constituted an important milestone for the development of the functional in the general-geometry form. A thermal-desorption experiment had been performed on this vdW model system and PAHs on graphite, largely for the purpose of providing benchmarks for possible relevant theories, with estimates of the experimental error [52].

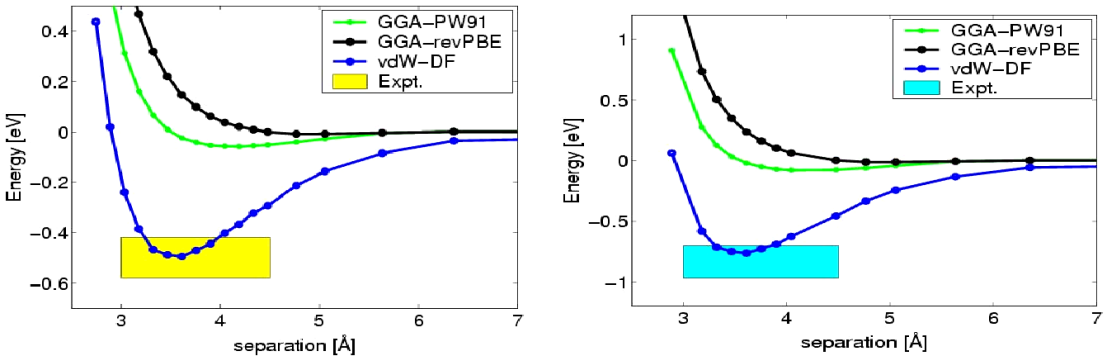

Figure 18. Benzene–graphene (left) and naphthalene–graphene (right) PECs [45], compared to experimental values for the desorption energy (heights of boxes accounting for error bars) [52].

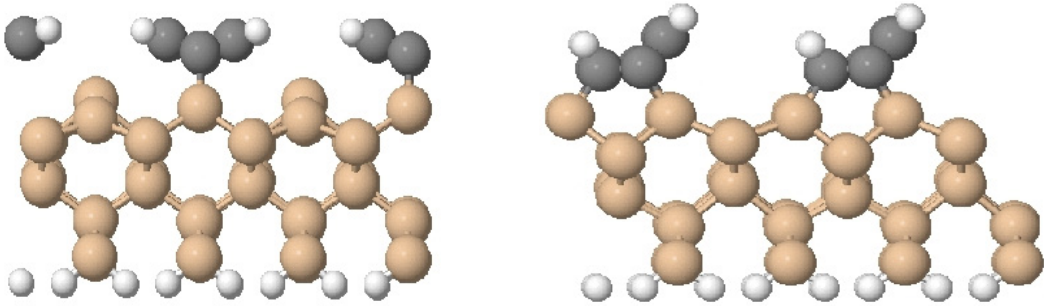

Figure 19. Butterfly (BF; left) and tight-bridge (TB; right) structures of C_6H_6 on Si(001)-(2 × 1), viewed along [$\bar{1}$10] [60].

The fact that the calculated PEC minima for both benzene and naphthalene on graphite (figure 18) fall within these error bars is promising for the vdW-DF method.

Adsorption of benzene has also been studied with vdW-DF on the Si(001)-(2 × 1) surface [60], where extensive studies with a variety of experimental tools have given conflicting results [60]. There is agreement on the two most stable structures, the butterfly (BF) and tight-bridge (TB) structures (figure 19), but to date none such on which is the stable one. Inclusion of vdW forces is found to make a *qualitative* difference to the results. Standard DFT with PBE or revPBE functionals finds that the TB structure is always stable, whereas vdW-DF calculations imply that, for some coverages, vdW forces stabilize the BF structure [60]. The results have significant implications for many DFT studies, as vdW forces are generally considered to have a negligible effect on covalently bonded systems and are usually ignored [60].

Adsorption of adenine on graphite has been studied with the vdW-DF as a response to a recent letter [61], where a semi-empirical approach is used. A semi-empirical vdW potential, a dipolar formula with damping functions caused by a cutoff on the dipolar singularity, has been proposed early on [62], and is now in extensive use [63, 24, 48, 61]. However, the 'procedure cannot be rigorously justified, although it is certainly more reasonable than the use of the [asymptotic] vdW potential where it is divergent' [62]. With no fitted parameters, the vdW-DF gives [39] (i) an adsorption energy of 0.7 eV (like experiment [61]), (ii) an equilibrium separation of 3.5 Å and (iii) a longitudinal optical phonon frequency in the *c* direction in graphite of 13 meV (experiment: 15.6 meV).

Phenol is a benzene molecule with one H atom replaced by an OH radical (figure 20). The adsorption of phenol (figure 20) [64] demonstrates a covalent bond to dominate on Al_2O_3, a vdW bond dominating on graphite and a metallic bond on nickel [65]. The vdW bond is ubiquitous but absent in the Ni PBE calculation of [65]. Preliminary results with the vdW-DF point at a weaker adsorption (0.41 eV) and even a different adsorption site [66].

Molybdenum sulfide (MoS_2) is a layered compound. Adsorption of aromatic and conjugated compounds on the basal plane of MoS_2 has been calculated with the vdW-DF [67] and shown to be well described in comparisons with available desorption data [68]. The benzene PEC (figure 21) looks very much like that for benzene on graphite (figure 18).

Morikawa *et al* [69] have used vdW-DF to study benzene adsorption on the (111) surfaces of Al, Cu, Ag and Au. While the binding energy for these systems is small within GGA (∼0.02 eV), it is found that the vdW contribution causes an order of magnitude increase. The adsorption geometry undergoes no change for the noble metal surfaces, although for Al the metal–molecule distance decreases by ∼15% when the vdW interaction is included. Comparison of calculated workfunction change vs. experimental values suggests that the metal–molecule distances are overestimated by both GGA and vdW-DF.

Applications of the vdW-DF [70] have been made to the adsorption of butane (C_4H_{10}) on metals, in particular n-butane on the (111) surfaces (figure 22) of Cu, Au and Pt [70], with GGA results from [71] and with experimental data

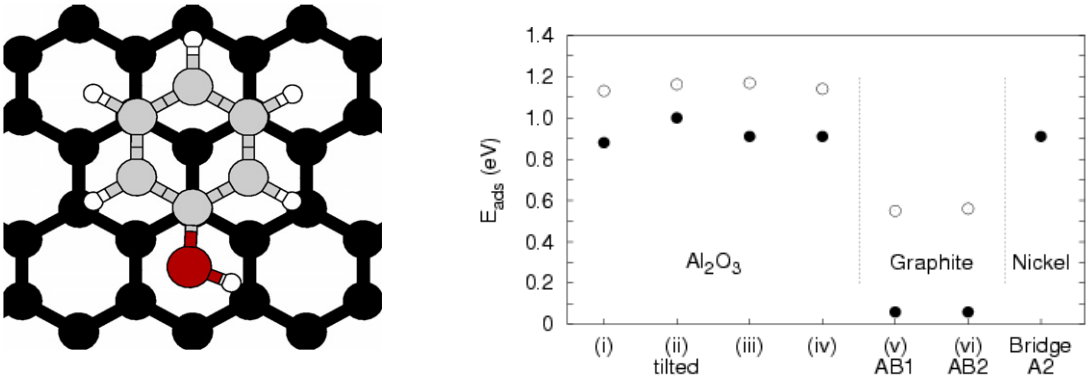

Figure 20. A phenol molecule symmetrically placed on a graphite surface (left). Phenol adsorption-energy values calculated with the vdW-DF method [2] for adsorption on Al_2O_3 and graphite, where covalent (GGA; filled circle) and covalent plus vdW (vdW-DF; empty circle) energy contributions are indicated [64] and with PBE for adsorption on Ni [65] are shown on the right.

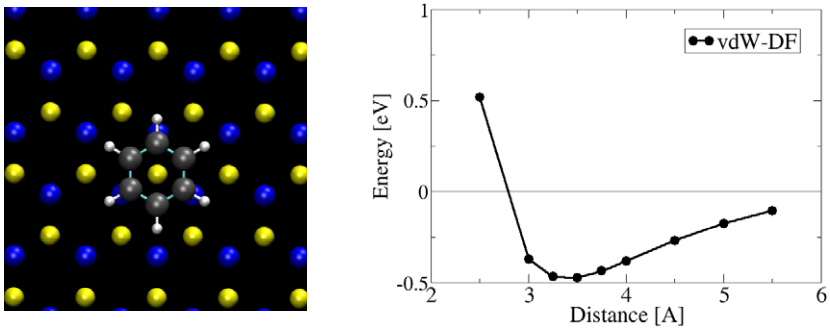

Figure 21. Benzene adsorption on the basal plane of MoS_2: geometry (left) and potential-energy curve (right) [67].

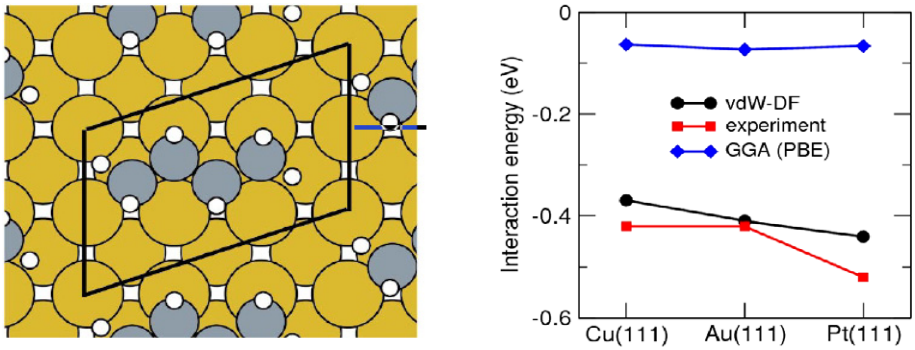

Figure 22. Adsorption structure and energy values for n-butane on Cu(111), Au(111) and Pt(111) [70]. GGA values [71] and experimental numbers [72–74] are shown for comparison. Left panel reprinted with permission from [71]. Copyright 2004 by the American Physical Society.

from [72–74]. The calculated and measured adsorption-energy values show good agreement in figure 22 [70].

Adsorption of thiophene on Cu(110) has recently been addressed in [75]. In this prototype case, relevant for organic field-emitter transistors (OFETs), the interface between metal and a π-conjugated molecule is of interest. In their vdW-DF calculation, the authors use RPBE, which they find to give results close to revPBE. The calculated adsorption energy is 0.26 eV. The variation of the inner potential is calculated with vdW-DF [75] and the workfunction with a thiophene overlayer is found to be 3.63 eV, as compared to the experimental value 3.65 eV, a substantial lowering of the clean Cu(110) surface value of 4.45 eV (figure 23).

The adsorption calculations have a favorable direct link to experimental adsorption-energy values, typically measured in desorption experiments. At large, comparisons with experiments indicate that the vdW-DF has a useful accuracy. An even more detailed assessment of vdW-DF can be made when experimental results for adsorption geometries and vibrational properties are available. The adsorption-induced change of the workfunction is another calculable quantity of key interest.

5.4. Interfaces

Alq3 (tris-(8-hydroxyquinoline)) is one of the most widely used materials in OLEDs. The barrier for injection is

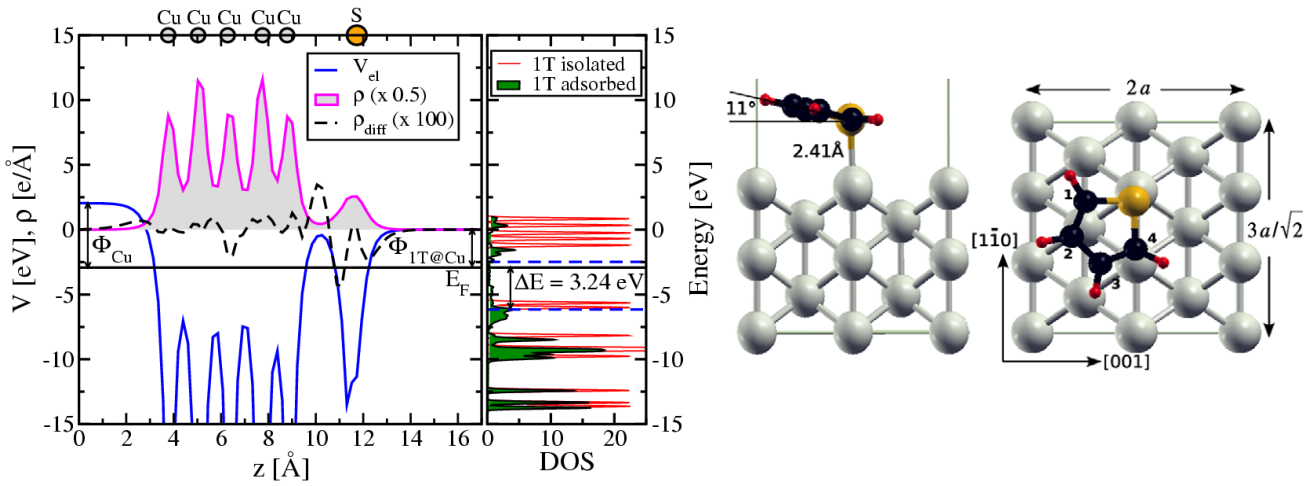

Figure 23. The calculated inner potential, charge-density profile and adsorbate-induced Kohn–Sham spectrum [75] (left). The adsorption structure (right) [75]. Reprinted with permission from [75]. Copyright 2008 by the American Physical Society.

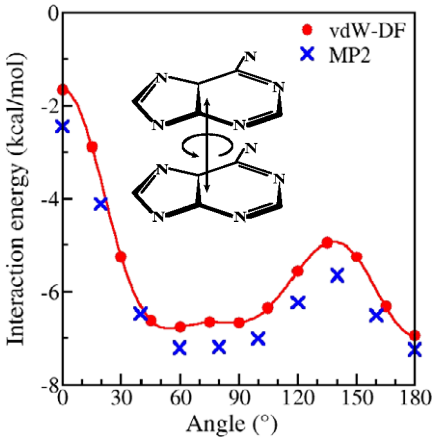

Figure 24. Adenine–adenine interactions in vdW-DF [78] compared with wavefunction calculations. vdW-DF calculations between all other combinations [78] show comparable or better agreement with the MP2 calculation than what is shown in the comparison above.

significantly altered by the Alq3/Al interfacial dipole layer, for which quite a number of origins have been proposed. This interfacial dipole when Alq3 is adsorbed on Al has been studied using vdW-DF [76]. Although binding energies obtained by ordinary functionals give a poor description, the bonding configurations are found to have correct binding energies when the vdW-DF is included, and one obtains interface dipoles that agree reasonably well with experimental results, including a decreased surface workfunction [76].

5.5. DNA

To understand the structures and forces behind the genetic code is a true challenge. In the nucleic acids the base-pair stacking is of key importance, and in cancer treatment DNA intercalation has a central role.

A briefing on DNA certainly includes the double helix of nucleic acids, which happens to be right handed in B-DNA, and also mentions RNA. DNA and RNA are connected by a sugar phosphate backbone, with specific pairing of nucleic acids. vdW-DF has been used to show that the stacking interactions between the neighboring base pairs, caused to a large degree by the vdW or London dispersion interactions, play an important role in defining the twist and rise from one base pair to the next, even in the absence of the sugar phosphate backbone.

Table 3. vdW-DF results for twist and rise in DNA [78].

	vdW-DF predictions	Nucleic acid database
Twist	$34° \pm 10°$	$36° \pm 7°$
Rise	3.5 ± 0.1 Å	3.3 ± 0.2 Å

For the stacking interactions of individual bases, the results are in good agreement between vdW-DF and MP2 calculations [77, 78, 46]. This applies to adenine–adenine (figure 24), cytosine–cytosine, guanine–guanine. uracil–uracil, adenine–cytosine, adenine–guanine, adenine–uracil, cytosine–guanine, cytosine–uracil and guanine–uracil pairs. Thymine–thymine, thymine–adenine, thymine–cytosine, thymine–guanine and thymine–uracil pairs form a special group.

In applications to stacked DNA base-pair duplexes (figure 25), the vdW-DF does as well on the hydrogen bond as PBE [77] and compares well with high-level calculations. Stacked base pairs are beyond the limits of standard quantum-chemical methods, except by partitioning the system into smaller units. The stacking energy versus twist of the several base-pair duplexes shown below is not practical to obtain by any other method.

The vdW-DF calculated values of the twist and rise [78] have a good overlap with the experimental ones [82] (table 3). The $\pm$ signs do not represent errors, but are rather the standard deviations caused by different sequence dependences.

In comparison with the best quantum-chemical calculations the vdW-DF results come out well (figure 26). Note that the vdW-DF calculations appear more accurate than the force field with many fitted parameters.

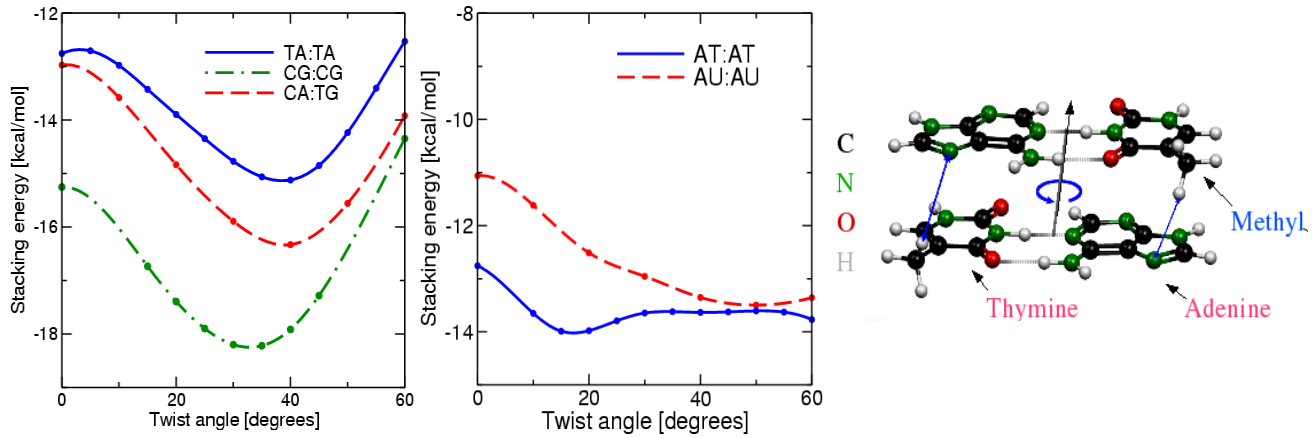

Figure 25. Typical vdW-DF stacking energy curves [78] for several base-pair duplexes of DNA are shown in the left panel. A couple are irregular, one of which is shown in the middle panel and illustrated in the right panel. The downward bump in the solid blue curve is caused by what appears to be an incipient hydrogen bond between the hydrogen of the methyl groups of thymine (T) with an unsaturated nitrogen on the adenines (A). In uracil (U), found in RNA instead of thymine, the methyl terminations are replaced by hydrogen ones, thus causing, as revealed by the dashed red curve, less binding and a partial rotational instability. The weakened binding in the RNA version is suggested by experiment [79–81].

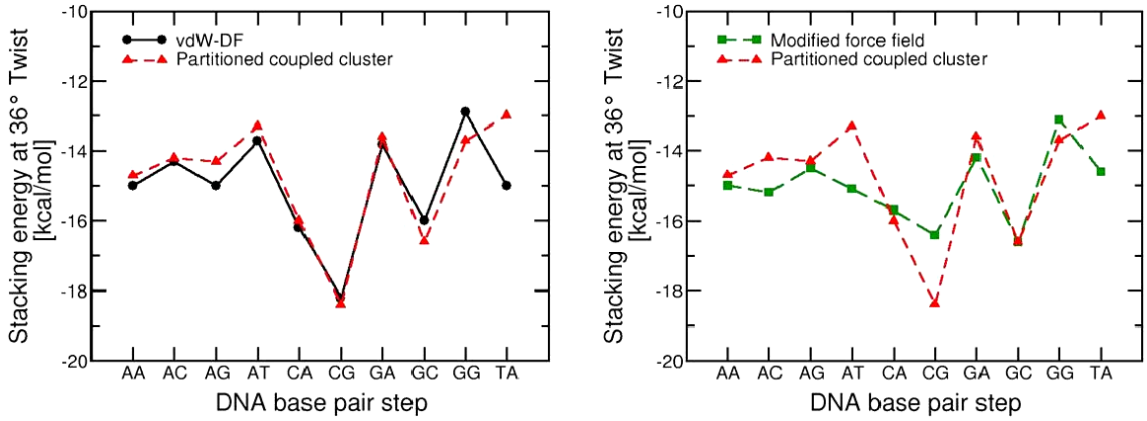

Figure 26. Comparison of vdW-DF results [78] with partitioned coupled cluster [83] (left) and Amber force field (modified [83] for better fit) with partitioned coupled cluster (right).

The DNA applications can be summed up as (i) vdW-DF gives good comparison with MP2 for stacked nucleic acids, (ii) it does not disturb the GGA's accurate description of the H-bond, (iii) it is able to easily model stacking interactions of base pairs and (iv) it is able to reveal insights related to the stabilizing effect of thymine within DNA. vdW-DF is thus an adequate and powerful method for modeling DNA.

Figure 27. Proflavine, a DNA intercalator and an antibacterial agent. The intercalating form of proflavine has a single positive charge, which is spread out rather uniformly through the aromatic rings, rather than concentrated on the central nitrogen as might be suggested by simple bond counting [84].

5.6. DNA intercalators

DNA intercalators are molecules that find their way between the stacked base pairs in DNA. They are mostly flat and aromatic. Their usefulness lies in drug design and drug action, e.g. chemotherapy drugs against cancer. They also have roles as antibacterial agents and DNA dyes. An example of a DNA intercalator is proflavine (figure 27). The most stable form is charged.

The interaction of proflavine and GC and AT pairs has been studied with vdW-DF [84], and the interesting results, like much smaller twist with proflavin present, might have biological consequences. This preference is observed experimentally in intercalators [85–88], specifically in proflavine [89], and it likely provides some impetus for the DNA to unwind enough to allow intercalation. It also has a stronger interaction with a neighboring base pair than they have with each other, perhaps a necessary condition for intercalation. The conclusion, that most binding comes from

dispersion, but that charge is necessary, e.g. for G:C to prefer proflavine over another G:C or C:G, is also interesting [84]. Qualitatively similar results were found for the three other combinations [84]. They all point at the vdW-DF method also being promising in this context.

6. Summary, conclusions and outlook

We have made an approximate DFT that includes van der Waals interactions (now also self-consistently). Correlation energy is divided into two pieces. The LDA is used to approximate the local-density piece. A simple dielectric function is used in the small nonlocal piece. A growing number of calculations on molecules and materials show that this vdW-DF has a useful accuracy.

The vdW-DF study is only in its beginnings. There are many more applications to do. The exchange functional, $E_x[n]$, calls for further studies. As the vdW interaction is out in the tails of orbitals, these need further study. The correlation functional, $E_c^{nl}[n]$, needs further study. Applications in molecular dynamics should be done.

The vdW-DF method shows promise to extend the broad successes of density-functional theory to new classes of matter. This is shown in several applications that cannot be done by any other nonempirical method.

Acknowledgments

Work at Rutgers was supported in part by the National Science Foundation (US) under grant DMR-045693 and by the Department of Energy (US) under grant DEFG02-08ER46471 via University of Texas at Dallas subcontract SC8-17. BIL gratefully acknowledges support from the Lundbeck foundation (Denmark) and the hospitality of Professor Hideaki Kasai and the 2nd International Conference on Quantum Simulators and Design.

References

[1] Rydberg H, Dion M, Jacobson N, Schröder E, Hyldgaard P, Simak S I, Langreth D C and Lundqvist B I 2003 *Phys. Rev. Lett.* **91** 126402
Rydberg H, Jacobson N, Hyldgaard P, Simak S I, Lundqvist B I and Langreth D C 2003 *Surf. Sci.* **532** 606
[2] Dion M, Rydberg H, Schröder E, Langreth D C and Lundqvist B I 2004 *Phys. Rev. Lett.* **92** 246401
Dion M, Rydberg H, Schröder E, Langreth D C and Lundqvist B I 2005 *Phys. Rev. Lett.* **95** 109902
[3] Thonhauser T, Cooper V R, Shen Li, Puzder A, Hyldgaard P and Langreth D C 2007 *Phys. Rev.* B **76** 125112
[4] Hohenberg P and Kohn W 1964 *Phys. Rev.* **136** B864
[5] Kohn W and Sham L J 1965 *Phys. Rev.* **140** A1133
[6] Lundqvist B I, Andersson Y, Shao H, Chan S and Langreth D C 1995 *Int. J. Quantum Chem.* **56** 247
[7] Gell-Mann M and Brueckner K A 1957 *Phys. Rev.* **106** 364
[8] Hedin L and Lundqvist B I 1971 *J. Phys. C: Solid State Phys.* **4** 2064
[9] von Barth U and Hedin L 1972 *J. Phys. C: Solid State Phys.* **5** 1629
[10] Gunnarsson O and Lundqvist B I 1976 *Phys. Rev.* B **13** 4274
[11] Ceperley D A and Alder B J 1980 *Phys. Rev. Lett.* **45** 566
[12] Ma S-K and Brueckner K A 1968 *Phys. Rev.* **165** 18
[13] Langreth D C and Mehl M J 1981 *Phys. Rev. Lett.* **47** 446
[14] Becke A D 1988 *Phys. Rev.* A **38** 3098
[15] Lee C, Yang Y and Parr R G 1988 *Phys. Rev.* B **37** 785
[16] Perdew J P, Chevary J A, Vosko S H, Jackson K A, Pederson M A, Singh D J and Fiolhais C 1992 *Phys. Rev.* B **46** 6671
[17] Becke A D 1993 *J. Chem. Phys.* **98** 5648
[18] Perdew J P, Burke K and Ernzerhof M 1996 *Phys. Rev. Lett.* **77** 3865
[19] Andersson Y, Langreth D C and Lundqvist B I 1996 *Phys. Rev. Lett.* **76** 1780
[20] Kohn W, Meir Y and Makarov D E 1998 *Phys. Rev. Lett.* **80** 4153
[21] Dobson J F and Wang J 1999 *Phys. Rev. Lett.* **82** 2123
[22] Langreth D C and Perdew J P 1975 *Solid State Commun.* **17** 1425
[23] Langreth D C and Perdew J P 1977 *Phys. Rev.* B **15** 2884
[24] Wu X, Vargas M C, Nayak S, Lotrich V and Scoles G 2001 *J. Chem. Phys.* **115** 8748
[25] Zhang Y and Yang W 1998 *Phys. Rev. Lett.* **80** 890
[26] Langreth D C, Dion M, Rydberg H, Schröder E, Hyldgaard P and Lundqvist B I 2005 *Int. J. Quantum Chem.* **101** 599
[27] Puzder A, Dion M and Langreth D C 2006 *J. Chem. Phys.* **126** 164105
[28] Vydrov O A, Wu Q and Van Voorhis T 2008 *J. Chem. Phys.* **129** 012106
[29] Dion M 2004 van der Waals forces in density functional theory *PhD Thesis* Rutgers University
[30] Li S, Cooper V R, Thonhauser T, Puzder A and Langreth D C 2008 *J. Phys. Chem.* A at press
[31] Chakarova-Käck S D, Kleis J and Schröder E 2008 private communication
[32] Thonhauser T, Puzder A and Langreth D C 2006 *J. Chem. Phys.* **126** 164106
[33] Feller D 1999 *J. Phys. Chem.* A **103** 7558
[34] Zhao Y, Tishchenko O and Truhlar D G 2005 *J. Phys. Chem.* B **109** 19046
[35] Jurecka P, Sponer J and Hobza P 2006 *Phys. Chem. Chem. Phys.* **8** 1985
[36] Hooper J, Cooper V C, Thonhauser T, Romero N A, Zerilli F and Langreth D C 2008 *ChemPhysChem* **9** 891
[37] Jacobson N, Tegner B, Schröder E, Hyldgaard P and Lundqvist B I 2002 *Comput. Mater. Sci.* **24** 373
[38] Hyldgaard P *et al* 2008 private communication
[39] Chakarova-Käck S D, Schröder E, Lundqvist B I, Cooper V R and Langreth D C 2008 private communication
[40] Ogilvie J and Wang F 1992 *J. Mol Struct.* **273** 277
[41] Chakarova-Käck S D 2006 Towards first-principles understanding of biomolecular adsorption *PhD Thesis* Chalmers University of Technology, Sweden
[42] Tsuzuki S, Honda K, Uchimaru T and Mikami M 2004 *J. Chem. Phys.* **120** 647
[43] Kleis J, Schröder E and Hyldgaard P 2008 *Phys. Rev.* B **77** 205422
[44] Sinnokrot M O and Sherrill C D 2004 *J. Am. Chem. Soc.* **126** 7690
[45] Chakarova-Käck S D, Schröder E, Lundqvist B I and Langreth D C 2006 *Phys. Rev. Lett.* **96** 146107
[46] Elstner M, Hobza P, Frauenheim T, Suhai S and Kaxiras E 2001 *J. Chem. Phys.* **114** 5149
[47] Cooper V C, Thonhauser T and Langreth D C 2008 *J. Chem. Phys.* **128** 204102
[48] Grimme S 2004 *J. Comput. Chem.* **25** 1463
[49] Grimme S, Anthony J, Schwabe T and Mück-Lichtenfeld C 2007 *Org. Biomol. Chem.* **5** 741
[50] Dobson J F, White A and Rubio A 2006 *Phys. Rev. Lett.* **96** 073201

[51] Benedict L X, Chopra N G, Cohen M L, Zettl A, Louie S G and Crespi V H 1998 *Chem. Phys. Lett.* **286** 490
[52] Zacharia R, Ulbricht H and Hertel T 2004 *Phys. Rev.* B **69** 155406
[53] Kleis J, Lundqvist B I, Langreth D C and Schröder E 2007 *Phys. Rev.* B **76** 100201
[54] Hyldgaard P *et al* 2008 private communication
[55] Ziambaras E, Kleis J, Schröder E and Hyldgaard P 2007 *Phys. Rev.* B **76** 155425
[56] Li J, Chabal Y and Langreth D C 2008 private communication
[57] Pan L, Sander M B, Huang X Y, Li J, Smith M, Bittner E, Bockrath B and Johnson J K 2004 *J. Am. Chem. Soc.* **126** 1308
[58] Lee J Y, Pan L, Kelly S R, Jagiello J, Emge T J and Li J 2005 *Adv. Mater.* **17** 2703
[59] Sagara T, Ortony J and Ganz E 2005 *J. Chem. Phys.* **123** 214707
[60] Johnston K, Kleis J, Lundqvist B I and Nieminen R M 2008 *Phys. Rev.* B **77** 121404
[61] Ortmann F, Schmidt W G and Bechstedt F 2005 *Phys. Rev. Lett.* **95** 186101
[62] Brooks F C 1952 *Phys. Rev.* **46** 92
[63] Halgren T A 1992 *J. Am. Chem. Soc.* **114** 7827
Elstner M, Hobza P, Frauenheim T, Suhai S and Kaxiras E 2001 *J. Chem. Phys.* **114** 5149
Wu Q and Yang W 2002 *J. Chem. Phys.* **116** 515
Hasegawa M and Nishidate K 2004 *Phys. Rev.* B **70** 205431
Zimmerli U, Parrinello M and Koumoutsakos P 2004 *J. Chem. Phys.* **120** 2693
[64] Chakarova-Käck S D, Borck Ø, Schröder E and Lundqvist B I 2006 *Phys. Rev.* B **74** 155402
[65] Delle Site L, Alavi A and Abrams A F 2003 *Phys. Rev.* B **67** 193406
[66] Kelkkanen A *et al* 2008 private communication
[67] Moses P G, Mortensen J J, Lundqvist B I and Nørskov J K 2008 private communication
[68] Salmeron M, Somorjai G A, Wold A, Chianelli R and Liang K S 1982 *Chem. Phys. Lett.* **90** 105
[69] Morikawa Y *et al* 2008 private communication
[70] Lee K 2008 private communication
[71] Morikawa Y, Ishii H and Seki K 2004 *Phys. Rev.* B **69** 041403
[72] Taplyakov A V, Gurevich A B, Yang M X, Bent B E and Chen J G 1998 *Surf. Sci.* **396** 340
[73] Wetterer S M, Lavrich D J, Cummings T, Bernasek S L and Scoles G 1998 *J. Phys. Chem.* B **102** 9266
[74] Weaver J F, Ikai M, Carlsson A and Madix R J 2001 *Surf. Sci.* **470** 226
[75] Sony P, Pusching P, Nabok D and Ambrosch-Draxl C 2008 *Phys. Rev. Lett.* **99** 176401
[76] Yanagisawa S, Lee K and Morikawa Y 2008 *J. Chem. Phys.* **128** 244704
[77] Cooper V R, Thonhauser T and Langreth D C 2008 *J. Chem. Phys.* **128** 204102
[78] Cooper V R, Thonhauser T, Puzder A, Schröder E, Lundqvist B I and Langreth D C 2008 *J. Am. Chem. Soc.* **130** 1304
[79] Ross P D and Howard F B 2003 *Biopolymers* **68** 210
[80] Howard F B 2005 *Biopolymers* **78** 221
[81] Soto A M, Rentzeperis D, Shikiya R, Alonso M and Marky L A 2006 *Biochemistry* **45** 3051
[82] Olson W K, Bansal M, Burley S K, Dickerson R E, Gerstein M, Harvey S C, Heinemann U, Lu X-J, Neidle S, Shakked Z, Sklenar H, Suzuki M, Tung C-S, Westhof E, Wolberger C and Berman H M 2001 *J. Mol. Biol.* **313** 229
[83] Šponer J, Jureka P, Marchan I, Luque F J, Orozco M and Hobza P 2006 *Chem. Eur. J.* **12** 2854
[84] Li S *et al* 2008 private communication
[85] Lerman L S 1961 *J. Mol. Biol.* **3** 18
[86] Bond P J, Landridge R, Jennette K W and Lippard S J 1975 *Proc. Natl Acad. Sci. USA* **72** 4825
[87] Shieh H-S, Berman H, Dabrow M and Neidle S 1980 *Nucleic Acids Res.* **8** 85
[88] Canals A, Purciolas M, Aymami J and Coll M 2005 *Acta Crystallogr.* D **61** 1009
[89] Schneider B, Ginell S L and Berman H 1992 *Biophys. J.* **63** 1572